

Electronic Supplementary Information

Complete furanics-sugar separations with metal-organic framework NU-1000

Mizuho Yabushita,^{ab} Peng Li,^c Hirokazu Kobayashi,^b Atsushi Fukuoka,^{*b} Omar K. Farha^{*cd} and Alexander Katz^{*a}

^a*Department of Chemical and Biomolecular Engineering, University of California, Berkeley, California 94720, United States*

^b*Institute for Catalysis, Hokkaido University, Sapporo, Hokkaido 001-0021, Japan*

^c*Department of Chemistry, Northwestern University, Evanston, Illinois 60208, United States*

^d*Department of Chemistry, Faculty of Science, King Abdulaziz University, Jeddah 22254, Saudi Arabia*

**Corresponding authors: fukuoka@cat.hokudai.ac.jp (AF); o-farha@northwestern.edu (OKF); askatz@berkeley.edu (AK)*

Table of Contents

1. Experimental	S3
2. Table S1 Langmuir parameters for furanics and sugars adsorption on NU-1000 at 297 K in single-component mode	S4
3. Fig. S1 Langmuir plots for HMF and furfural adsorption on NU-1000 in single mode.....	S4
4. Fig. S2 Single-component adsorption isotherms of furanics and sugars on MSC-30.	S5
5. Fig. S3 Langmuir plots for furanics and sugars adsorption on MSC-30 in single mode.....	S5
6. Table S2 Langmuir parameters for furanics and sugars adsorption on MSC-30 in single mode at 297 K.....	S6
7. Fig. S4 PXRD patterns of NU-1000 before and after furanics adsorption.	S6
8. Fig. S5 N ₂ physisorption data of NU-1000 before and after HMF adsorption.	S7
9. Fig. S6 N ₂ physisorption data of NU-1000 before and after furfural adsorption.....	S7
10. Table S3 Decrease in pore volume of NU-1000 after furanics adsorption.....	S8
11. Fig. S7 Langmuir plots for HMF and furfural adsorption on NU-1000 in competitive mode.	S8
12. Table S4 Langmuir parameters for furanics and sugars adsorption on NU-1000 at 297 K in competitive mode	S9
13. Fig. S8 Competitive adsorption of furanics and sugars on MSC-30.	S9
14. Table S5 Langmuir parameters for furanics and sugars adsorption on MSC-30 in competitive mode at 297 K	S10
15. Fig. S9 Langmuir plots for HMF and furfural adsorption on MSC-30 in competitive mode.	S10
16. Table S6 Adsorption ratios of furanics to sugars for reported adsorbents.....	S11
17. References	S11

Experimental

1. Synthesis and characterization of NU-1000

The NU-1000 MOF was synthesized by following the reported procedure.^{S1} Powder X-ray diffraction (PXRD) data were collected on a Rigaku model ATX-G diffractometer equipped with a Cu rotating anode X-ray source. N₂ physisorption isotherm measurements were performed on a Micromeritics Tristar II 3020 (Micromeritics, Norcross, GA) at 77 K. Between 30 and 50 mg of material was used for each measurement.

2. Aqueous-phase adsorption of furanics and sugars on NU-1000

To investigate adsorption of furanics and sugars on NU-1000 in aqueous solution, five compounds were employed: 5-hydroxymethylfurfural (HMF); furfural; glucose; fructose; and xylose, which were supplied from Sigma-Aldrich and Acros Organics. An aqueous stock solution containing single component (for single-component adsorption) or multicomponent (for competitive-mode) with high concentration was prepared in a volumetric flask. The stock solution was used as-is or after dilution in Milli-Q water (18 MΩ cm). 5 mg of NU-1000 was dispersed in 1.5 mL of the aqueous solution. We also tested another adsorbent, commercial mesoporous carbon material MSC-30 (Kansai Coke & Chemicals) and carbon black BP2000 (Cabot). The suspension was ultrasonicated for 1 min to disperse the adsorbent well, vortexed for at least 30 min at 297 K, and then filtered with a syringeless filter device Mini-UniPrep equipped with a polytetrafluoroethylene membrane (0.2 μm mesh, Whatman). The amount of residual compound in the liquid-phase filtrate was quantified by high-performance liquid chromatography (HPLC, Shimadzu, Prominence HPLC System, refractive index detector) equipped with an Aminex HPX-87H column (Bio-Rad, ø7.8 × 300 mm, mobile phase 5 mM H₂SO₄ 0.6 mL min⁻¹, column temperature 323 K), with an absolute calibration method. The subtraction of mass of furanic/sugar detected by HPLC from that of compound charged gave an uptake.

All isotherms observed in this study exhibit Type I behavior (*i.e.*, Langmuir isotherm), except for glucose, fructose, or xylose on NU-1000 (see Figs. 1 and 2) or such sugars on MSC-30 (see Fig. S8). The Langmuir equation [Eq. (S1)] gives the adsorption equilibrium constant (K_{ads}) and adsorption capacity (Q_{max}) for each isotherm.

$$Q = \frac{CK_{\text{ads}}Q_{\text{max}}}{1 + CK_{\text{ads}}} \quad (\text{S1})$$

where C is the equilibrium concentration and Q is the uptake. This equation is transformed into Eq. (S2), which represents the Langmuir plot.

$$\frac{C}{Q} = \frac{C}{Q_{\text{max}}} + \frac{1}{K_{\text{ads}}Q_{\text{max}}} \quad (\text{S2})$$

Table S1 Langmuir parameters for furanics and sugars adsorption on NU-1000 at 297 K in single-component mode

Adsorbate	Langmuir parameter	
	$K_{\text{ads}}^a / \text{M}^{-1}$	$Q_{\text{max}}^b / \text{mg g}_{\text{NU-1000}}^{-1}$
HMF	120 ± 16	240 ± 3
Glucose	No adsorption	0
Fructose	No adsorption	0
Furfural	28 ± 6	467 ± 28
Xylose	No adsorption	0

^a Adsorption equilibrium constant. ^b Adsorption capacity.

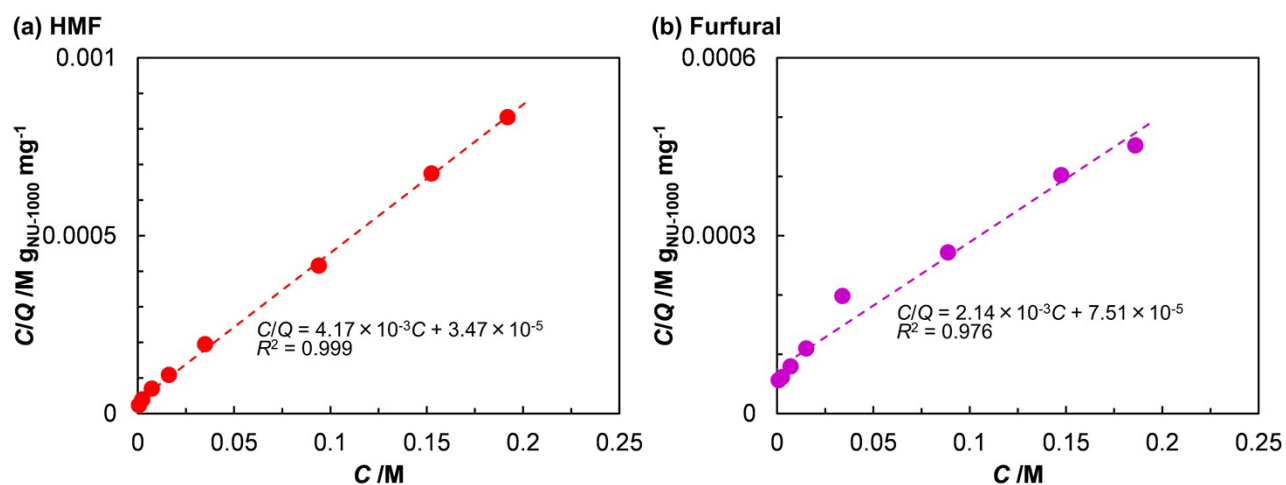


Fig. S1 Langmuir plots for HMF and furfural adsorption on NU-1000 in single mode, from the isotherms recorded at 297 K (Fig. 1). The estimated Langmuir parameters are summarized in Table S1.

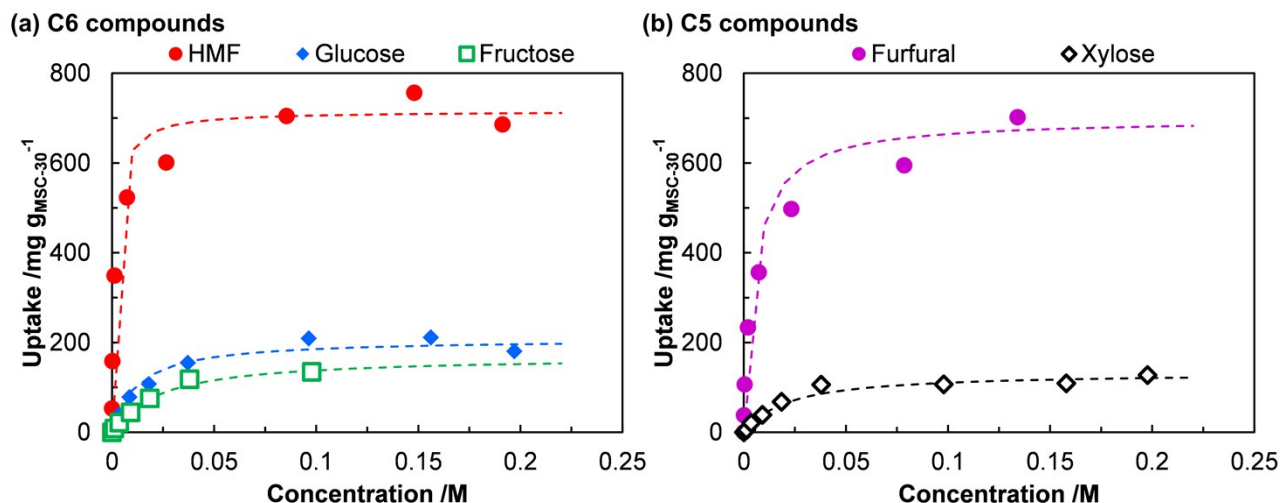


Fig. S2 Single-component adsorption isotherms of furanics and sugars on MSC-30, recorded at 297 K: (a) C6 compounds; (b) C5 compounds. The dashed lines represent the isotherms replicated by the Langmuir parameters (Table S2). The Langmuir plots are shown in Fig. S3.

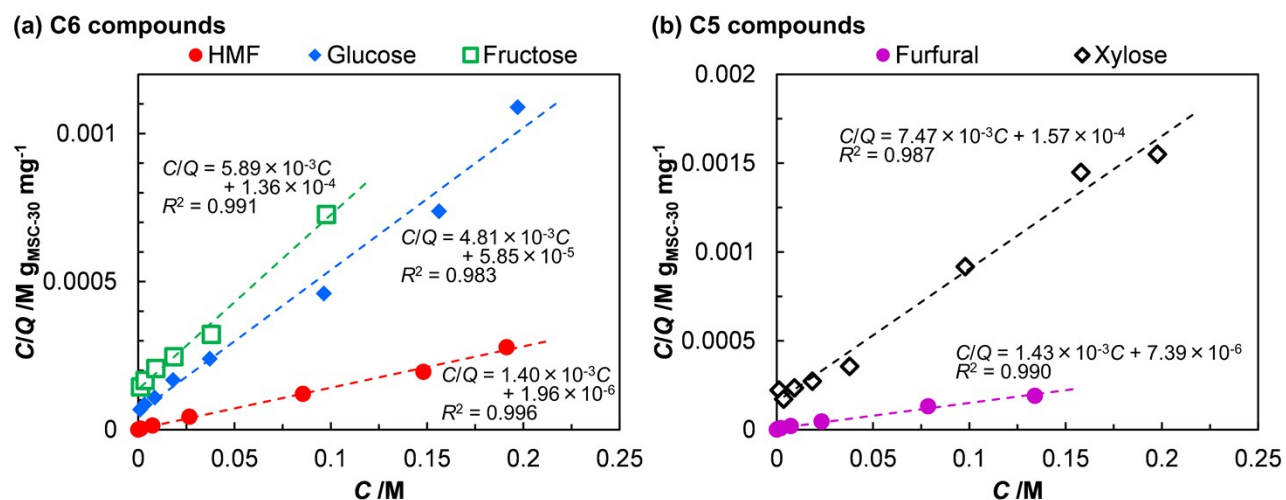


Fig. S3 Langmuir plots for furanics and sugars adsorption on MSC-30 in single mode, from the isotherms recorded at 297 K (Fig. S2). The estimated Langmuir parameters are summarized in Table S2.

Table S2 Langmuir parameters for furanics and sugars adsorption on MSC-30 in single-component mode at 297 K

Adsorbate	Langmuir parameter	
	$K_{\text{ads}}^a / \text{M}^{-1}$	$Q_{\text{max}}^b / \text{mg g}_{\text{MSC-30}}^{-1}$
HMF	714 ± 450	716 ± 18
Glucose	82 ± 28	208 ± 11
Fructose	43 ± 5	170 ± 8
Furfural	194 ± 71	699 ± 30
Xylose	47 ± 10	134 ± 6

^a Adsorption equilibrium constant. ^b Adsorption capacity.

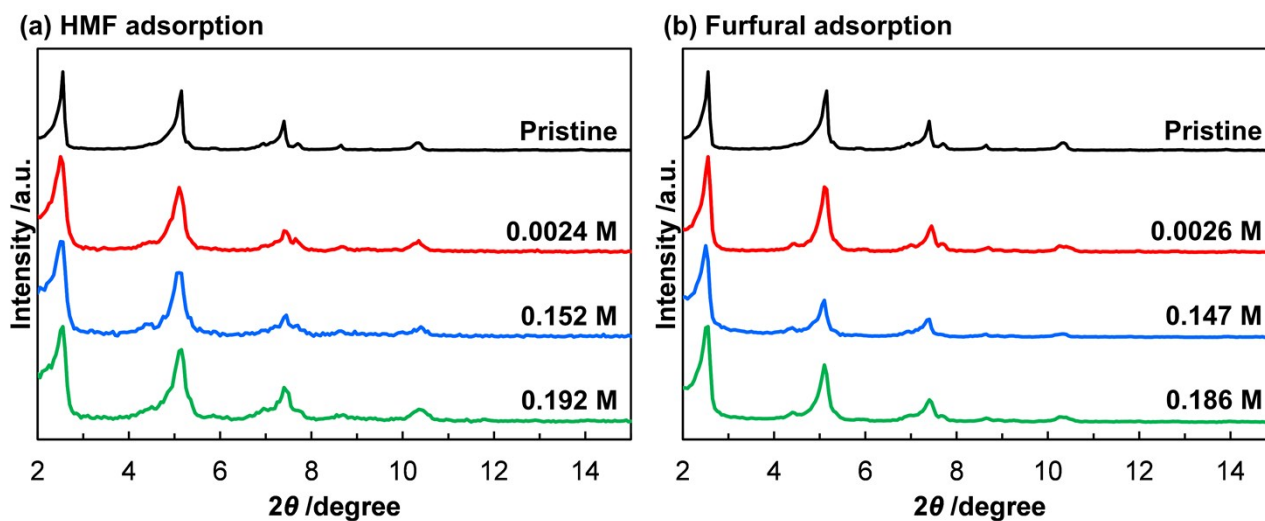


Fig. S4 PXRD patterns of NU-1000 before and after furanics adsorption: (a) HMF adsorption and (b) furfural adsorption.

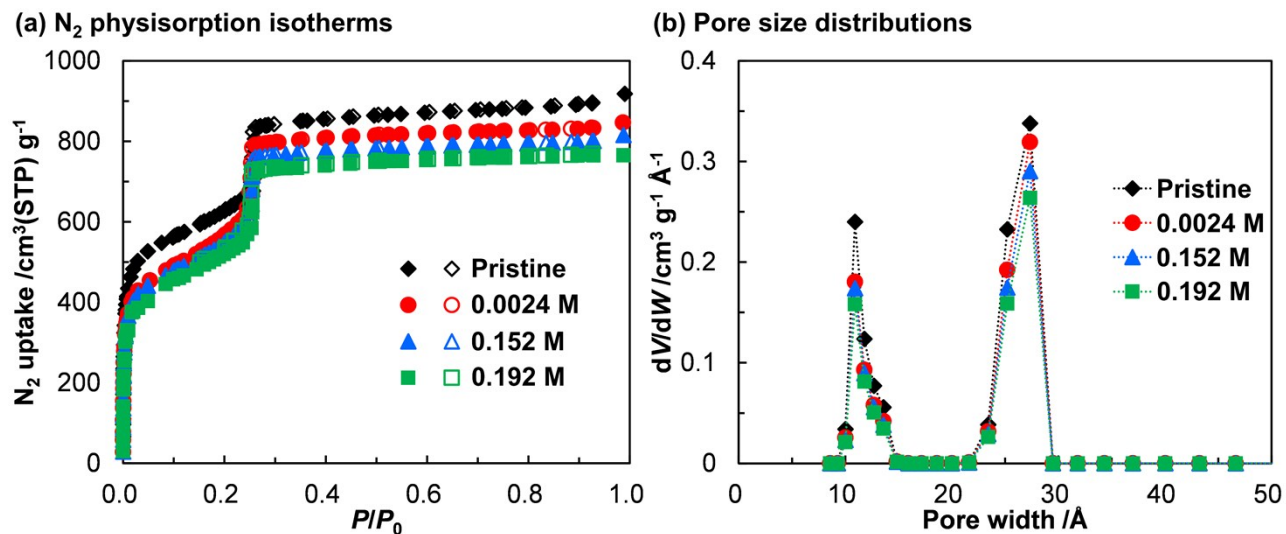


Fig. S5 N₂ physisorption data of NU-1000 before and after HMF adsorption, recorded at 77 K: (a) isotherms and (b) pore size distributions. In Fig. S5a, closed dots represent adsorption branch, and open dots do desorption branch. The concentrations shown in the figures represent the equilibrium concentration values in solution, and can be converted to adsorbed furanics concentrations on the solid with isotherm data of Fig. 1.

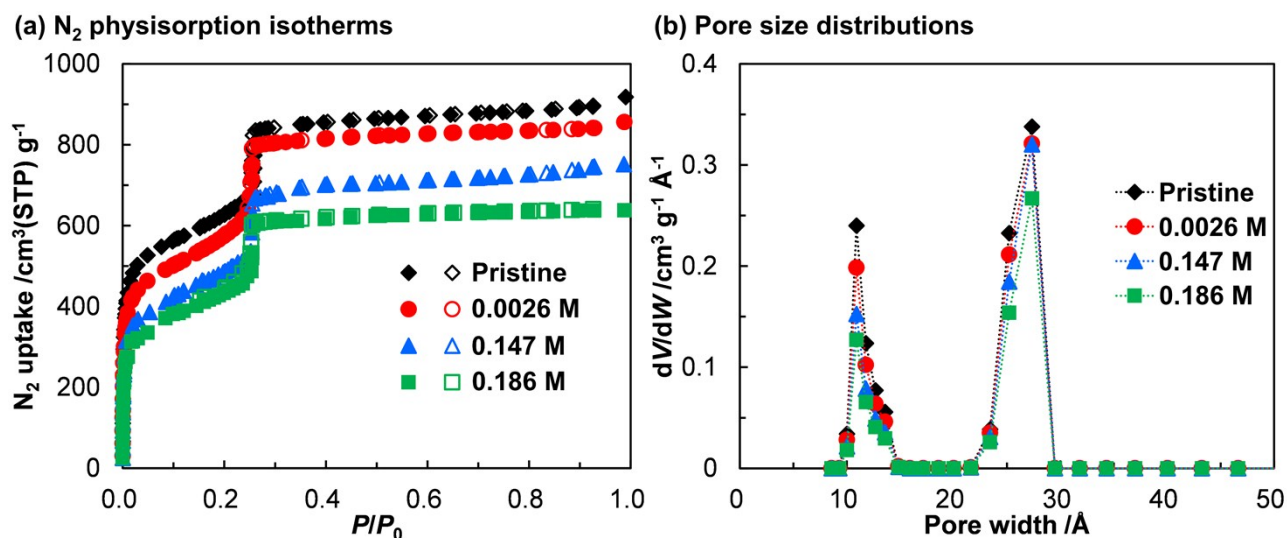


Fig. S6 N₂ physisorption data of NU-1000 before and after furfural adsorption, recorded at 77 K: (a) isotherms and (b) pore size distributions. In Fig. S6a, closed dots represent adsorption branch, and open dots do desorption branch. The concentrations shown in the figures represent the equilibrium concentration values in solution, and can be converted to adsorbed furanics concentrations on the solid with isotherm data of Fig. 1.

Table S3 Decrease in pore volume of NU-1000 after furanics adsorption

Adsorbate	C^a /M	Adsorbed furanics volume /cm ³ g _{NU-1000} ⁻¹	Pore volume change ^b /cm ³ g _{NU-1000} ⁻¹		
			Micropore	Mesopore	Total
HMF	0.0024	0.046	−0.120	−0.132	−0.252
HMF	0.152	0.174	−0.137	−0.233	−0.370
HMF	0.192	0.178	−0.169	−0.326	−0.495
Furfural	0.0026	0.027	−0.084	−0.084	−0.168
Furfural	0.147	0.240	−0.176	−0.146	−0.322
Furfural	0.186	0.269	−0.227	−0.330	−0.557

^a Equilibrium concentration. ^b Difference between pore volume of NU-1000 before and after furanics adsorption, determined from N₂ physisorption measurement.

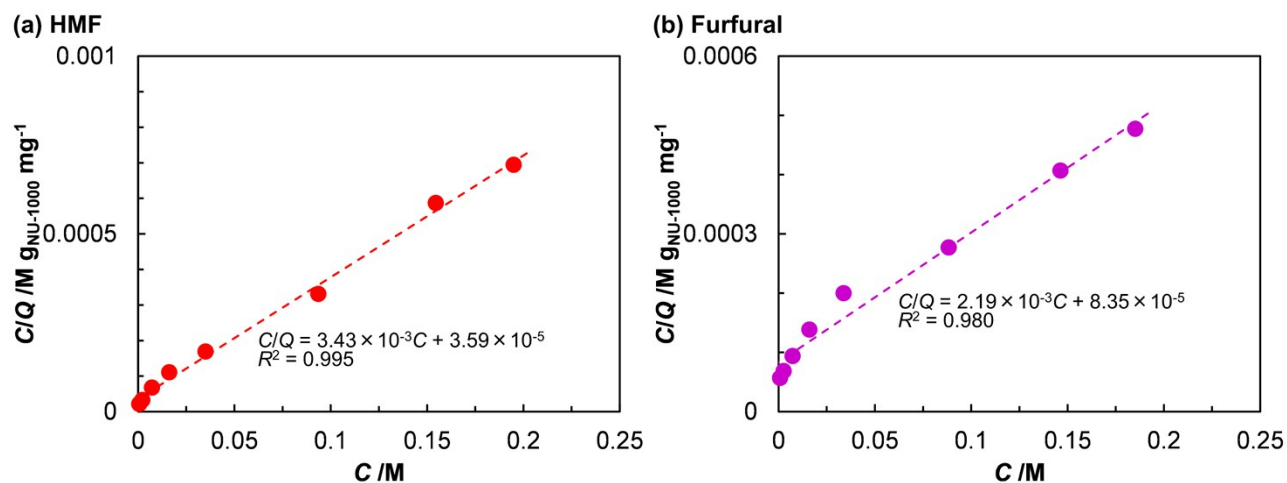


Fig. S7 Langmuir plots for HMF and furfural adsorption on NU-1000 in competitive mode, from the isotherms recorded at 297 K (Fig. 2). The estimated Langmuir parameters are summarized in Table S4.

Table S4 Langmuir parameters for furanics and sugars adsorption on NU-1000 at 297 K in competitive mode

Adsorbate	Langmuir parameter	
	$K_{\text{ads}}^a / \text{M}^{-1}$	$Q_{\text{max}}^b / \text{mg g}_{\text{NU-1000}}^{-1}$
HMF	96 ± 21	292 ± 8
Glucose	No adsorption	0
Fructose	No adsorption	0
Furfural	26 ± 5	457 ± 25
Xylose	No adsorption	0

^a Adsorption equilibrium constant. ^b Adsorption capacity.

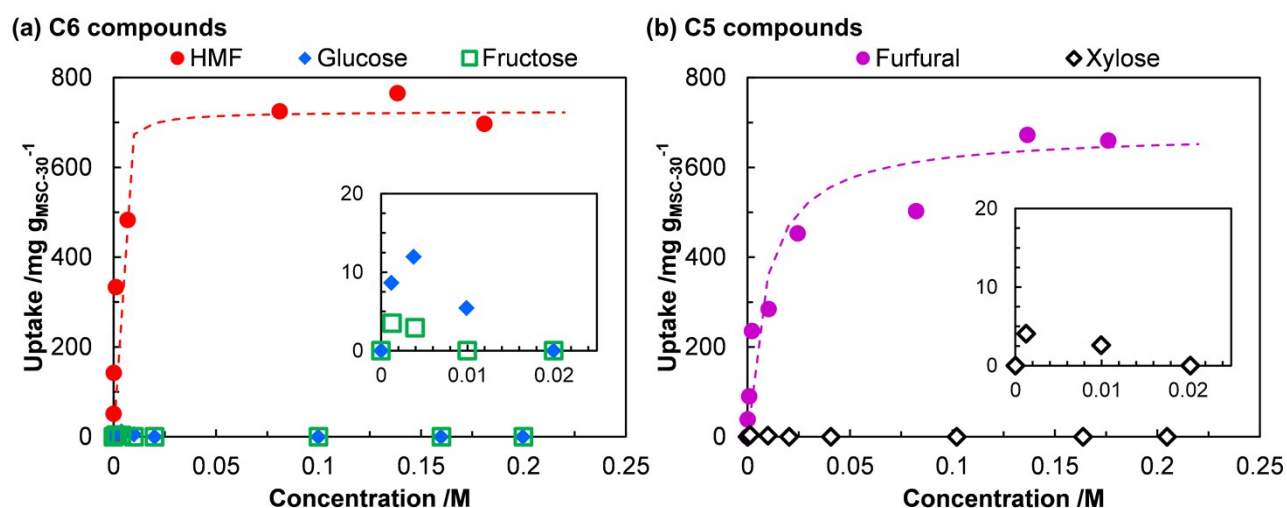


Fig. S8 Competitive adsorption of furanics and sugars on MSC-30, recorded at 297 K: (a) C6 compounds; (b) C5 compounds. The insets represent the expanded figures in the range from 0 M to 0.02 M. The dashed lines represent the isotherms replicated by the Langmuir parameters (Table S5). The Langmuir plots for HMF and furfural are shown in Fig. S9.

At high HMF/furfural concentration, all adsorption sites of MSC-30 are occupied by these furanics, which thus inhibits sugars adsorption. However, in the case of high MSC-30 loading and/or low HMF concentration, sugars adsorb on the surface, in addition to HMF (see Figs. 3 and S10).

Table S5 Langmuir parameters for furanics and sugars adsorption on MSC-30 in competitive mode at 297 K

Adsorbate	Langmuir parameter	
	$K_{\text{ads}}^a / \text{M}^{-1}$	$Q_{\text{max}}^b / \text{mg g}_{\text{MSC-30}}^{-1}$
HMF	1312 ± 1000	725 ± 18
Glucose	n.d. ^c	n.d. ^c
Fructose	n.d. ^c	n.d. ^c
Furfural	113 ± 43	678 ± 35
Xylose	n.d. ^c	n.d. ^c

^a Adsorption equilibrium constant. ^b Adsorption capacity. ^c Not determined, due to non-Langmuir type adsorption isotherm.

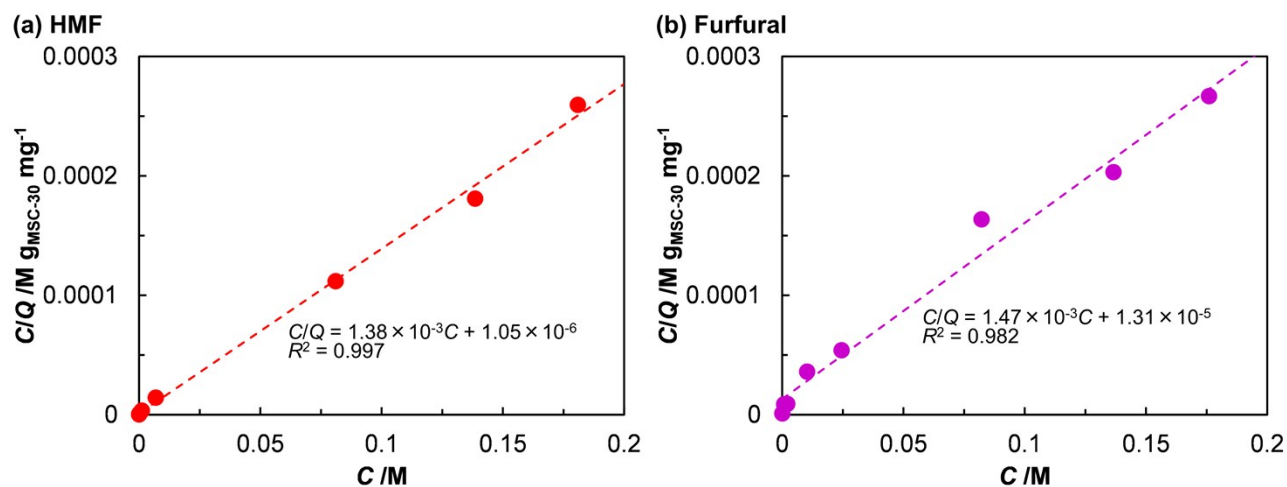


Fig. S9 Langmuir plots for HMF and furfural adsorption on MSC-30 in competitive mode, from the isotherms recorded at 297 K (Fig. S8). The estimated Langmuir parameters are summarized in Table S5.

Table S6 Adsorption ratios of furanics to sugars for reported adsorbents

Adsorbent	Adsorbate	Temp. /K	Adsorbent-solution ratio /g L ⁻¹	Furanics-sugars ratio ^a	Reference
NU-1000	HMF, glucose, fructose	297	3.3	∞	This work
NU-1000	HMF, glucose, fructose	297	33 ^e	∞	This work
MSC-30	HMF, glucose, fructose	297	33 ^e	1.4	This work
BP2000	HMF, glucose, fructose	297	33 ^e	2.1 ^f	This work
BP2000	HMF, fructose, levulinic acid	298	20	16 ^g	S2
ROX-N30 ^b	HMF, fructose, levulinic acid	296	20	25 ^h	S3
Hyperscrosslinked polymer ^c	HMF, fructose	293	20	7	S4
Hyperscrosslinked polymer ^c	HMF, fructose	n.d. ^d	20	23	S5

^a Ratio of furanic to sugar, based on adsorbed mass. ^b Activated carbon, oxidized by nitric acid.

^c Synthesized via Friedel-Crafts alkylation of 4,4'-bis(chloromethyl)-1,1'-biphenyl. ^d No data.

^e Competitive adsorption data are shown in Fig. 3. ^f The infinite ratio of HMF to fructose can be achieved only when HMF occupies all adsorption sites of BP2000. We should note that BP2000 exhibits fructose uptake in single-component adsorption experiment, and this behavior is contrast to the complete lack of fructose adsorption on NU-1000 even in the absence of HMF (see Fig. 1).

^g Levulinic acid of *ca.* 100 mg was also adsorbed on 1 g of BP2000. ^h Levulinic acid of *ca.* 10 mg was also adsorbed on 1 g of ROX-N30.

References

- S1 T. C. Wang, N. A. Vermeulen, I. S. Kim, A. B. F. Martinson, J. F. Stoddart, J. T. Hupp and O. K. Farha, *Nat. Protocols*, 2016, **11**, 149.
- S2 P. Dornath and W. Fan, *Microporous Mesoporous Mater.*, 2014, **191**, 10.
- S3 P. Vinke and H. van Bekkum, *Starch/Stärke*, 1992, **44**, 90.
- S4 C. Detoni, C. H. Gierlich, M. Rose and R. Palkovits, *ACS Sustainable Chem. Eng.*, 2014, **2**, 2407.
- S5 K. Schute and M. Rose, *ChemSusChem*, 2015, **8**, 3419.